

ORIGINAL ARTICLE

Open Access



Effect of Loading and Beam Sizes on the Structural Behaviors of Reinforced Concrete Beams Under and After Fire

Eunmi Ryu, Yeongsoo Shin and Heesun Kim*

Abstract

Performance-based fire resistance design needs consideration of various influencing parameters of structures such as load levels and cross-sectional size. Therefore, the studies of fire damaged reinforced concrete (RC) structures are performed experimentally and analytically. Twelve RC beams with different load levels and cross sections are exposed to high temperatures following the ISO 834 standard time temperature. After the fire test, the fire-damaged beams are loaded using four-point loading to obtain its residual strength. In addition, ABAQUS 6.10-3 is used to preform structural analyses of the ductility of the fire-damaged beams. The results indicate that the temperature, stiffness and ductility of the fire-damaged beams are significantly influenced by the load level, cross-sectional size and time exposed to fire. Also, the ductility of the fire-damaged beam can be predicted using an analytical method, which is not easy to otherwise determine experimentally.

Keywords: fire, RC beam, load level, cross sectional size, experimental study, analytical model

1 Introduction

Although reinforced concrete structures are extensively used due to their well-known thermal resistance, deterioration after exposure to fire includes a loss in strength and elastic modulus, cracking, and spalling of the concrete. Also, the structural system of a building can be unexpectedly damaged due to the complexity of the structural fire resistance properties. Therefore, it is important to investigate the thermal characteristics and structural behavior of fire-damaged RC structures to understand their load bearing capacity and safety.

The performance of structures during a fire has been actively studied by researchers using material experiments, structural tests and finite element (FE) analyses. The material properties, including the specific heat, conductivity, density and thermal expansion of concrete have been studied under high temperatures (Harmathy 1970, 1993). The material properties of high-strength concrete were reported by Kodur and Sultan (2003) and Cheng

et al. (2004). Jau and Huang (2008) investigated the behavior of corner columns under axial loading, biaxial bending and asymmetric fire loading. Fire tests were conducted on high-strength concrete columns exposed at elevated temperatures to investigate including temperature distributions and spalling between parameters such as cross sectional areas, cover thicknesses, and arrangements of reinforced bars by Shin et al. (2011). The study showed that temperature distributions increase with the increase of cross sectional area and the number of reinforcing bars but decrease with the increase of cover thickness. Wu et al. (2014) investigate the effect that cracks have on temperature distributions of concrete members in a fire. A recent study by Kang et al. (2016) investigated the effect of the thickness on the temperature distribution of reinforced concrete walls during a fire and investigated the effect of the moisture content on the thermal behavior of concrete walls. In addition, Choi et al. (2010, 2012) proposed an analytical approach to predict the temperature distribution and deformation of structural members. Parametric analyses were performed to examine the effects of the material properties on the thermal and structural behavior of fire-damaged

*Correspondence: hskim3@ewha.ac.kr

Department of Architectural and Urban Systems Engineering, 52, Ewhayeodae-gil, Seodaemun-gu, Seoul 03760, Republic of Korea
Journal information: ISSN 1976-0485 / eISSN 2234-1315

concrete members (Lamont et al. 2001; Hsu et al. 2006; Ryu et al. 2015). The finite element analyses of the CFRP-strengthened RC T-beams and RC beams reinforced with internal GFRP bars are performed by Hawileh et al. (2009, 2011) and Hawileh and Naser (2012) using the commercial software ANSYS to investigate the transfer mechanism. In their studies, it has been concluded that the performance of the beams exposed to fire loading can be accurately predicted. Nonetheless, it is necessary to understand influencing parameters because there are many factors that can influence structural behavior of structures exposed to fire and these studies can be used as basic data for performance resistance fire design.

This paper experimentally and analytically investigates the thermal characteristics and structural behavior of concrete beams according to loading and cross sectional size. Fire tests and residual strength tests are performed on RC beams with different load levels and cross sections to measure the temperature and residual strength. In addition, the ductility is analytically determined, and the analytical results are validated by comparing them to those obtained experimentally.

2 Experimental and FE Modeling Approach

2.1 Test Specimens and Variables

Twelve RC beams are fabricated with normal-strength concrete as listed in Table 1. For the experiments, the variables include time, beam size and loading, which corresponds to the fire exposure time period, cross-section size and initial load level, respectively. The width, depth and length of the specimens are 250 mm × 400 mm × 5000 mm, and 300 mm × 500 mm × 5000 mm and 350 mm × 650 mm × 5000 mm, as illustrated in Fig. 1. The beams were loaded with different load levels of 40, 60

and 80% of their nominal moment capacity (M_n), which corresponds to 4.82, 7.23 and 9.65 tonf for small beams, 10.88 tonf for middle beam and 28.99 tonf for large beam, respectively. All beams are designed to have the same reinforcement ratio and the number of rebars is changed according to the cross-section sizes. The beams are reinforced with three, five and seven steel bars with 19 mm of diameter for S, M and L series of the tested beams, respectively. In addition, stirrups of 10 mm diameter are used to prevent shear failure, as shown in Fig. 1.

All beams are cured for 4 months and are preheated at a low temperature to prevent a moisture effect during the fire test.

2.2 Materials

The proportion of concrete mix is based on that in Table 2. After 28 days of curing, the mean compressive strength of the concrete obtained from the tests is 25.08 MPa, and the mean tensile strength of the concrete is measured to be 2.98 MPa, as listed in Table 2. The yield strength and elastic modulus of all reinforcement (rebar and stirrup) are 448 MPa and 205 GPa, respectively, as listed in Table 3.

2.3 Test Set Up and Data Measurement

2.3.1 Fire Test and Residual Strength Test

Before heating, all beams are simply supported with an effective span of 4700 mm and subjected to a four-point loading system. The distance between the loading points is 1200 mm. The fire tests are performed in a heating chamber, as shown in Fig. 2. After the load reaches its designated load level, heat is applied to the beams and the load is maintained. All beams are heated on three surfaces according to ISO 834 standard time–temperature curve, as illustrated in Fig. 3 (ISO 834 1999).

Table 1 List of specimens.

Specimen	Size (width × depth × length)	Fire exposure time period (min)	Load level (%)	Load (tonf)
CONT	250 × 400 × 5000 (S series)	–	–	–
P1-60		60	40	4.82
P1-90		90	40	4.82
P1-120		120	40	4.82
P2-60		60	60	7.23
P2-120		120	60	7.23
P3-60	300 × 500 × 5000 (M series)	60	80	9.56
P3-120		120	80	9.56
MCONT		60	–	–
MP1-60	350 × 650 × 5000 (L series)	120	40	10.31
LCONT		60	–	–
LP1-60		120	40	18.79

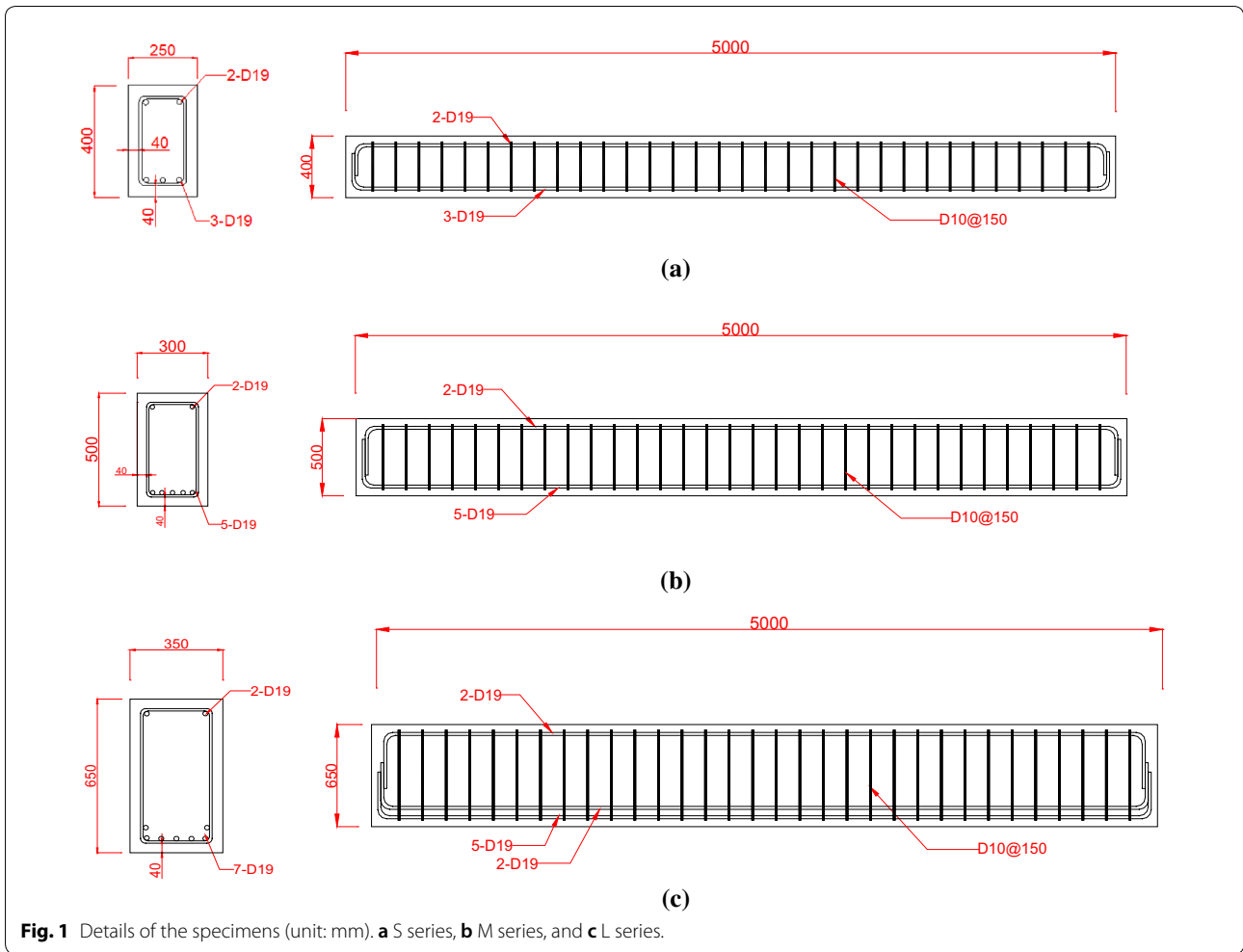


Table 2 material properties and mixture ratio for concrete.

28-day compressive strength (MPa)	28-day tensile strength (MPa)	W/C (%)	s/a (%)	Weight per unit volume (kg/m ³)				
				W	C	S	G	FA
25.08	2.98	53.4	49.8	83	155	913	914	1.86

Table 3 Material properties of steel.

Steel bar	Tensile strength (MPa)	Elastic modulus (GPa)
D19	448	205

After the fire test, the specimens are left for 1 week. For the residual strength test, all beams are subjected to the four-point bending test until the beam shows failure, as shown in Fig. 4.

2.3.2 Data Measurement

The vertical displacement during the fire test and residual strength test is obtained with a linear variable differential transformer (LVDT) located at the center of



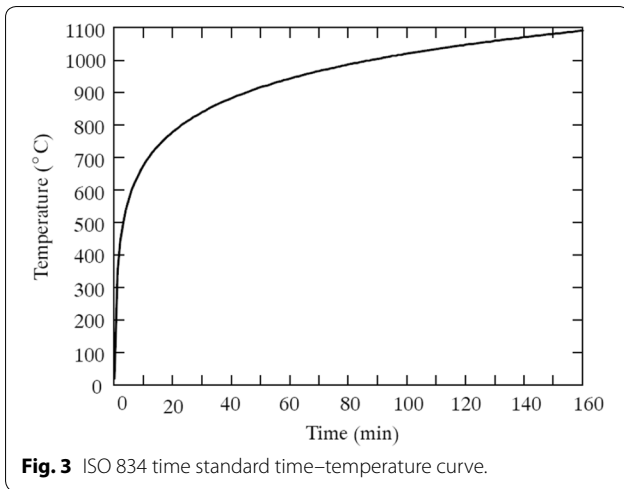


Fig. 3 ISO 834 time standard time-temperature curve.



Fig. 4 Residual strength test.

the beam length, as illustrated in Fig. 5. Electric strain gauges are attached at the upper and side surfaces of all beams to measure the strain of the concrete. The temperatures inside the S series beams are measured using six thermocouples within the beam section of the center and the temperatures of M series and L series beams are

measured using seven thermocouples within the beam section of the center. The locations of the thermocouples within the beam section can be found in Fig. 6. When possible, the strains of rebar are obtained for the gauges placed at the center rebar of the beams for the residual strength tests.

2.4 FE Modeling Approach

A high temperature has a significant influence on the ductility of the concrete beams. The ductility of the fire-damaged beam can be calculated using the deflection of the yielding point and the ultimate deflection.

The ductility can be defined as the ability of the fire-damaged beams to sustain large deformations before reaching failure. In particular, the fire damaged beams show brittle behavior compared to non-damaged beams, even if the maximum load capacity does not decrease significantly. Therefore, it is important to examine the beam for brittle behavior through the ductility index. The deflection ductility index is calculated based on Eq. (1) (Ashour 2000; Rashid and Mansur 2005).

$$\mu_{\Delta} = \Delta_u / \Delta_y \tag{1}$$

where μ_{Δ} is the deflection ductility index, Δ_u is the mid-span deflection at the ultimate beam load, and Δ_y is the midspan deflection at the yielding load of the tensile rebar.

However, the strains of the rebar in some beams cannot be obtained due to the construction environment. Therefore, structural analyses are conducted for the beams under the same conditions as those of the experiment to provide the yield point of the rebars. ABAQUS version 6.10-3, a commercial FE software, is used for FE analyses. FE analyses are conducted to know yielding point of rebar on the fire damaged beam. The temperature distributions obtained from the experiments are assigned to the FE models with their corresponding material properties for

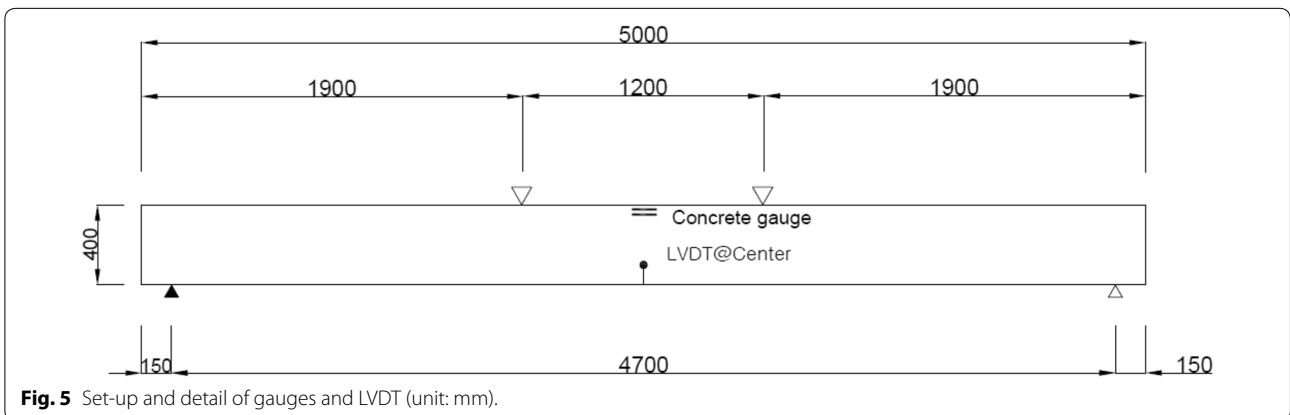
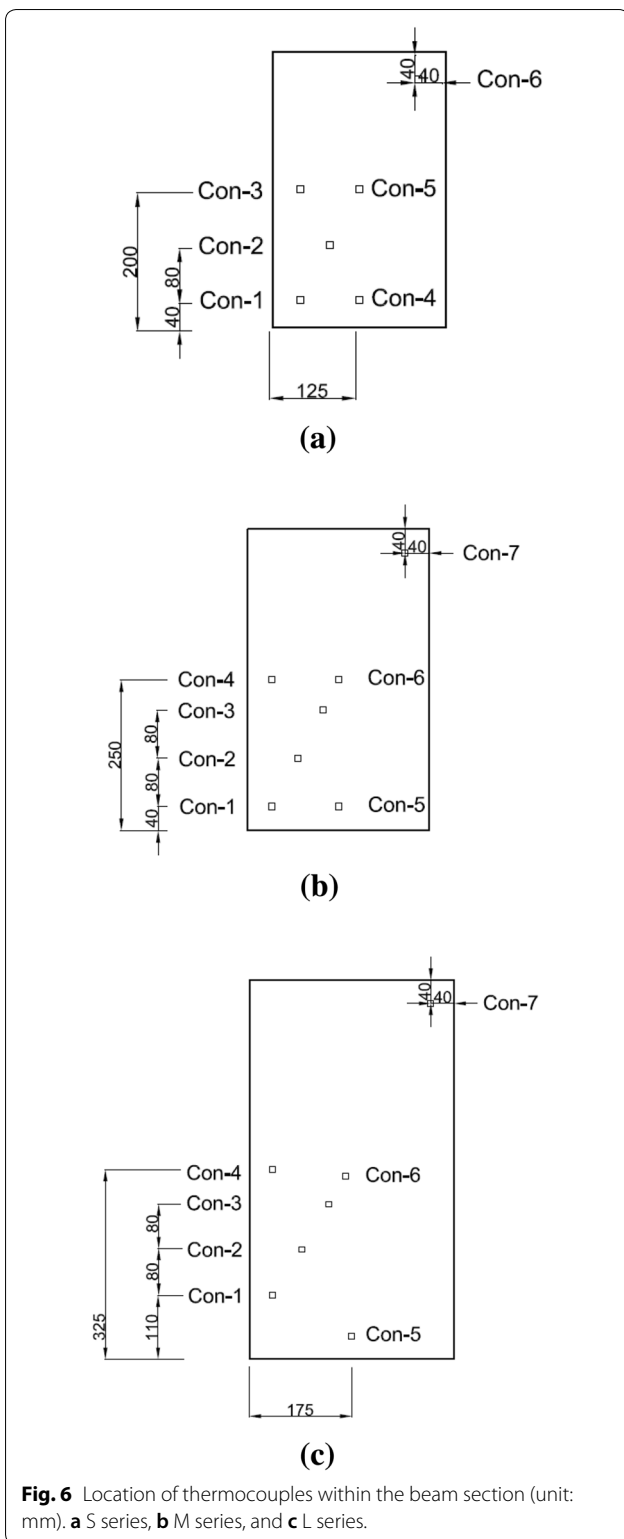


Fig. 5 Set-up and detail of gauges and LVDT (unit: mm).



performing structural analyses. FE models are generated with three-dimensional eight-node solid elements, having width, depth and length equal to the experimental conditions. Elements for the reinforcing steel bars are included in the model by assigning steel material properties to the meshes where the steel bars are located, as illustrated in Fig. 7a. The rest of the elements are modeled with concrete material properties.

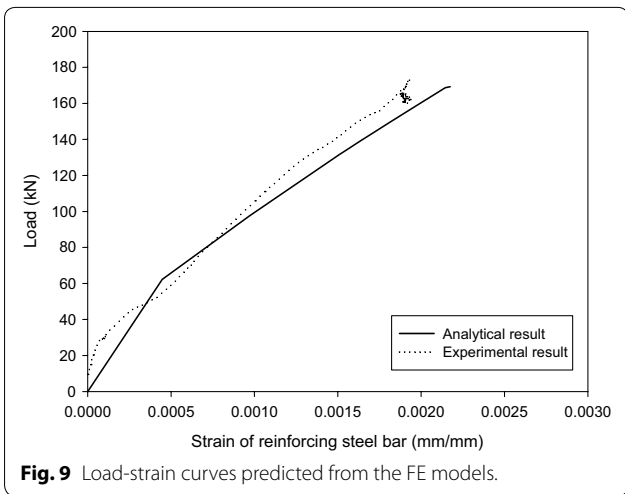
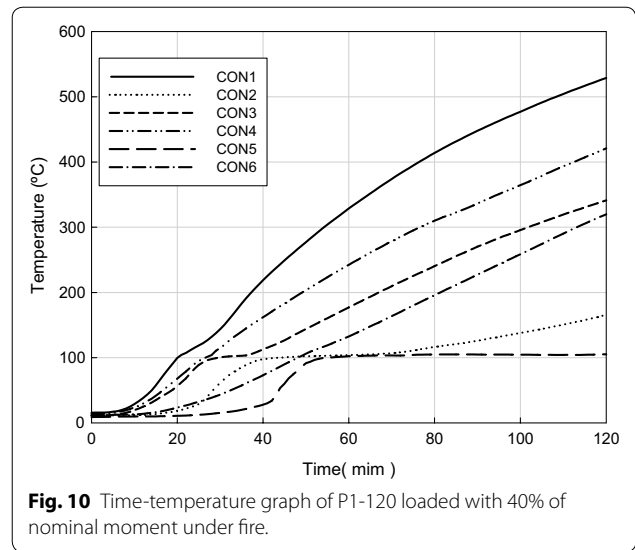
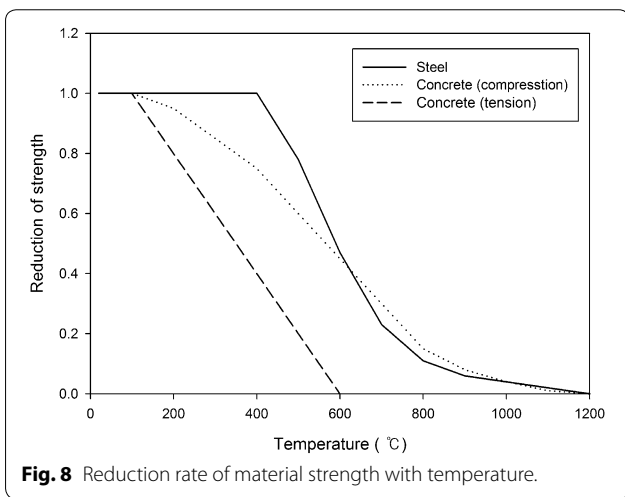
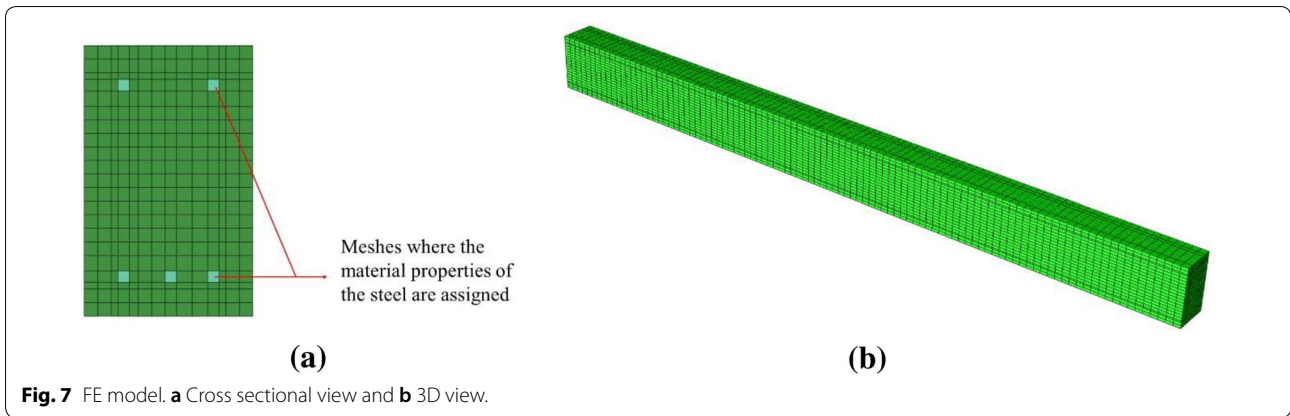
Loading and boundary condition are prescribed as in the experimental condition such that the RC beams are simply supported with a roller support at one side and a hinged support at the other side. In addition, loads are applied by displacement control. The variation of the elastic modulus, the compressive and tensile strength with temperature for the concrete and steel are modelled according to Eurocode 2 (1995). Reduction factors of strength of concrete and steel at the elevated temperatures can be obtained as illustrated in Fig. 8 by adopting the code.

The prediction of load-strain curve for the control beam from the FE model shows good agreements with that of the experimental results, as illustrated in Fig. 9. Then, the modeling approaches are implemented to the structural analyses to predict ductility of the fire damaged beams.

3 Results

3.1 Results of Fire Test

The experimental results show that the temperatures obtained from the thermocouples range from 100 to 600 °C depending on the location within the beam section. The time-temperature graph for P1-120 in Fig. 10 shows that the temperatures increase rapidly until 20 min of the fire test. However, after 20 min the temperature increase slows down. Time-temperature curves tend to be similar in the other specimens. The highest temperatures are obtained from the thermocouples among CON1, 3 and 4 of S series beams and CON1, 4 and 5 of M series and L series beams. All of these temperatures are located at 40 mm away from the fire exposed surface. The highest temperature increases as the load increases, as shown in Table 4 because the beam loaded with a high ratio of nominal moment causes more cracks and it is easier for the heat to be transferred through the cracks. However, differences in the highest temperature are not significant between beams with different cross-sectional sizes.



The maximum deflection of the beams during the fire test increases as the load level increases. However, the maximum deflection during the fire test decreases as the cross-sectional size increases, and the reduction ratio is not linearly proportional to the cross-sectional sizes. This is because there is combined effect of cross sectional sizes and temperature distributions on the deflection of the beams under fire. Figure 11 shows that the deflections of all specimens increase rapidly up to 20 min. After 60 min, the differences in the deflection between the specimens are larger. The maximum deflection of the beams is obtained at about 90 mm at the center of P3-120 loaded with 80% of nominal moment, which is three times larger than that of

Table 4 The highest temperatures and maximum deflection during a fire test.

Specimen	The highest temperature (°C)	Maximum deflection (mm)
CONT	–	–
P1-60	239	19.4
P1-90	523.6	30.9
P1-120	528.9	28.2
P2-60	214.1	18.7
P2-120	568.8	79.4
P3-60	312.1	37.3
P3-120	663.2	93.1
MCONT	–	–
MP1-60	352.0	19.1
LCONT	–	–
LP1-60	272.5	9.1

P1-120 loaded with 40% of nominal moment. The maximum deflections for P1-60 and MP1-60 are similar. The reason of having similar deflections between MP1-60 and P1-60 may be because of the combined effect of cross sectional sizes and temperature distributions. Even though MP1-60 has the larger cross sectional size, it also shows the higher temperature distributions than P1-60. The maximum deflection of LP1-60 is obtained at about 9.14 mm at the center of the beam, which is half that of P1-60.

3.2 Results of Residual Strength Test

3.2.1 Load Bearing Capacity

The load–deflection curves of all specimens obtained from the residual strength test are illustrated in Fig. 12. The differences in the maximum loads are small between all specimens because the temperatures of the reinforcing bars do not reach to 500 °C while the strength of steel are significantly reduced to 50% of the original strength. For specimens heated for 120 min, the maximum load of P1-120, P2-120 and P3-120 are 169.88, 172.96 and 161.58 kN, respectively. The differences between the maximum loads of the control beam and the other beam are within 10% such that the difference between the maximum loads of the control beam and P3-120 is the largest at 6.6%. The differences between the maximum load of control beams and the fire-damaged beams decreases as the cross-section size increases (Fig. 12).

3.2.2 Initial Stiffness

As shown in the load–deflection curves for the specimens, no significant difference can be found in the residual strength of the specimens. However, the slopes for the fire-damaged beams are considerably different. Therefore, the initial stiffness of the beams is compared to the load level, cross-sectional size and time (Sullivan et al. 2004). The stiffness decreases as the load level or time increases, as listed in Table 5. The stiffness of the fire-damaged beams decreases because of the material degradation of the concrete and steel with the increasing temperature, such as reduction of elastic modulus. The stiffness reduction ratio of the fire-damaged beam heated for 1 h is the largest, and the reduction ratio of the stiffness over time decreases. The stiffness for P1-60, P1-90 and P1-120 are 31, 42 and 44% less than that of the control beam, respectively.

As listed in Table 5, the stiffness decreases linearly as the load level increases. The stiffness for the P1-60, P2-60 and P3-60 beams are respectively 31, 37 and 43% less than that of the control beam.

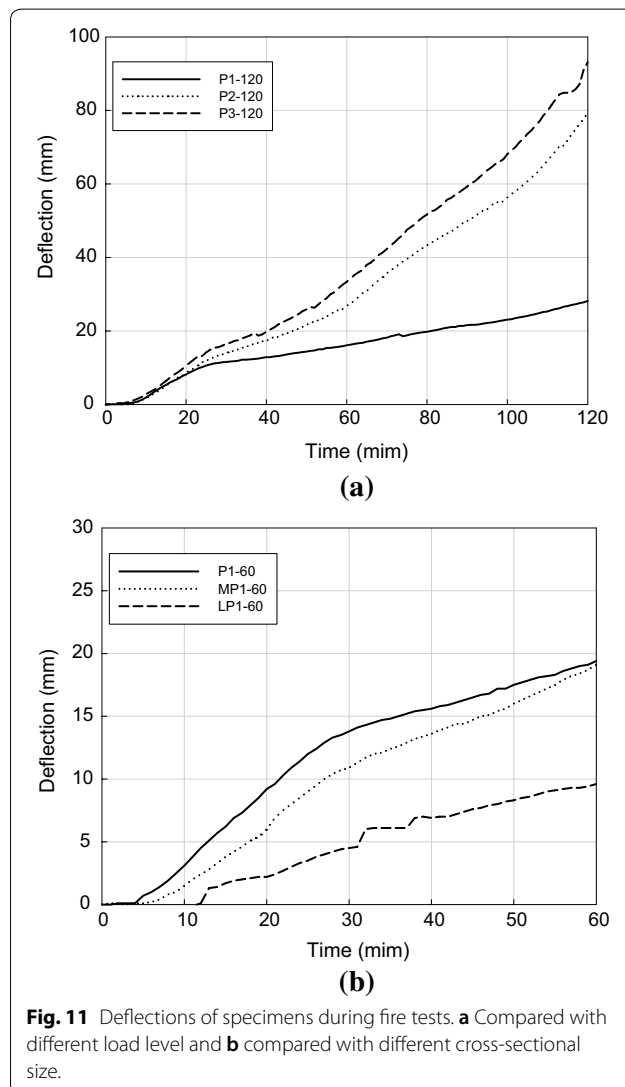


Fig. 11 Deflections of specimens during fire tests. **a** Compared with different load level and **b** compared with different cross-sectional size.

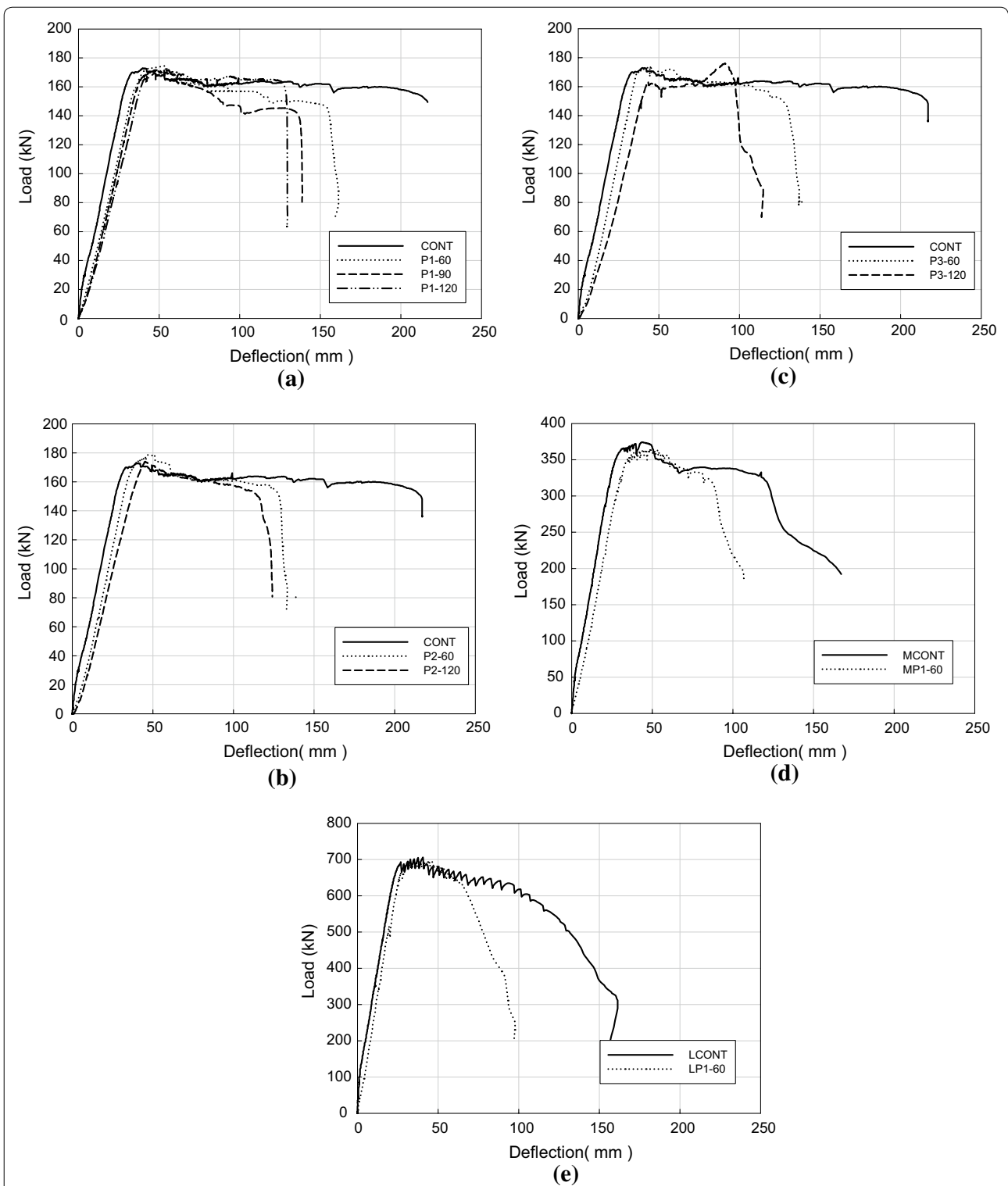


Fig. 12 Load-deflection curves for specimens. **a** Specimens of S series loaded with 40% of nominal moment, **b** specimens S series loaded with 60% of nominal moment, **c** specimens S series loaded with 80% of nominal moment, **d** specimens of M series, and **e** specimens of L series.

Table 5 Temperatures and deflection during the fire test.

Specimen	Stiffness (kN/mm)	Stiffness ratio
CONT	5.85	1.00
P1-60	4.05	0.69
P1-90	3.38	0.58
P1-120	3.28	0.56
P2-60	3.69	0.63
P2-120	2.91	0.50
P3-60	3.36	0.57
P3-120	2.51	0.43
MCONT	14.93	1.00
MP1-60	10.25	0.69
LCONT	33.32	1.00
LP1-60	24.74	0.77

The decrease rate is not proportional to the cross-sectional size. The stiffness for P1-60, MP1-60 and LP1-60 are 31, 31 and 23% less than that of the control beam, respectively. The stiffness of the S series are similar to the M series, but are different to the L series because the ratio of the area exposed to the high temperature to the entire cross-sectional area is small. As P1-60 and MP1-60 show similar deflections to each other, the stiffness of P1-60 and MP1-60 are similar due to the combined effect of cross sectional sizes and temperature distributions. Even though MP1-60 has the larger cross sectional size, it also shows the higher temperature distributions than P1-60. The results show that the stiffness of the beams is heavily influenced by the temperature.

3.2.3 Ductility

Fire-damaged beams exhibit brittle behavior compared to the control beam, as shown in Table 6. The

Table 6 Deflection ductility index of beams.

Specimen	Yielding load of rebar (kN)	Δ_y (mm)	Strain of yielding load of rebar	Δ_u (mm)	Ductility index (μ_Δ)
CONT	163.12	30.00	0.002382	216.20	7.21
P1-60	152.66	32.48	0.003019	154.23	4.75
P1-90	151.68	34.43	0.003483	135.35	3.93
P1-120	149.11	35.83	0.003488	127.56	3.56
P2-60	151.95	32.11	0.003454	127.86	3.98
P2-120	148.61	36.42	0.003504	115.82	3.18
P3-60	151.81	32.69	0.003499	118.74	3.63
P3-120	146.49	38.99	0.003536	97.78	2.51
MCONT	331.80	25.00	0.002382	121.10	4.84
MP1-60	302.71	27.60	0.002520	89.20	3.23
LCONT	685.51	32.00	0.002380	109.00	3.41
LP1-60	610.32	24.00	0.002954	68.40	2.85

ductility decreases as the load or the time exposed to fire increase, and the decrease rate is not proportional to the fire exposure time period. The difference in the ductility between the control beam and the beam heated for 1 h is higher than the difference between beams heated for 1 and 2 h. For the beam loaded with 40% of the nominal moment, the ductility indices for P1-60, P1-90 and P1-120 are 34.11, 45.44 and 50.59% less than that of control beam, respectively. For a beam loaded with 60% of the nominal moment, the ductility indices of P2-60 and P2-120 are 44.75 and 55.88% less than that of the control beam, respectively. For a beam loaded with 80% of the nominal moment, the ductility indices of P3-60 and P3-120 are 49.65 and 65.18% less than that of the control beam, respectively. Also, the ductility decreases as the load level increases because the temperature distribution inside the beam increases with the load level. For the beams heated for 2 h, the ductility of P1-120, P2-120 and P3-120 are 50.59, 55.88 and 65.18% less than that of control beam, respectively.

The ductility increases as the cross-sectional size increases. As shown in Table 6, the ductility descending of the control beams occurs as the cross-sectional size increases. However, the ratio of the ductility descending decreases as the cross-sectional size increases. The ductility indices for P1-60, MP1-60 and LP1-60 are respectively 34.11, 33.28 and 16.33% less than that of the control beam. The beam with a larger cross-sectional size can be seen to be more resistant to fire in terms of the maximum load as well as ductility.

The results show that the ductility of the beams is heavily influenced by fire even though the beams have small differences in the maximum load because the elastic modulus descending of concrete and steel according to temperature have more influence on the ductility, but the tensile strength decrease for the reinforcing bars related to maximum load is insignificant until 500 °C.

From FE analysis, it is possible to predict the ductility of the fire damaged beams and the predicted ductility indices show a reasonable tendency, compared with stiffness ratios.

4 Conclusions

This study investigated the thermal characteristics and structural behavior of beams exposed to fire according to load levels and cross sectional sizes. The following conclusions can be drawn.

- (1) In the experiments, the temperatures obtained from thermocouples range from 100 to 600 °C depending on the location within the cross section of the

beam. The results indicate that the temperature distributions increase as the load level increases, which can be explained by crack propagations due to loading. Therefore, predictions using FE methods can capture such behavior by adjusting the conductivity of the concrete depending on the load levels.

- (2) The deflection of the beams during the fire tests increases as the load level increases. However, the maximum deflection of the beams during fire test decreases nonlinearly as the cross section increases.
- (3) From residual strength tests of the fire damaged beams, differences in the maximum loads are not significant between all specimens because the temperatures of reinforcing bars did not reach 500 °C for the strength of steel to be reduced to 50% of the original strength. The difference between the maximum loads of the control beam and P3-120 is the largest.
- (4) The ductility and stiffness decrease as the load or time exposed to fire increase. Regarding different cross-sectional sizes, the ductility and stiffness of the beams are improved as the size of the cross section increases.
- (5) Further studies are needed to investigate weighted values among different influencing factors including cross-sectional size, load level and time exposed to fire for the fire-damaged RC beams.

Authors' contributions

ER carried literature study, conducted experiments, and drafted the manuscript. YS contributed in designing the experiments including the test variables. HK analyzed the test results and revised the manuscript. All authors read and approved the final manuscript.

Acknowledgements

This research was supported by a Grant (17CTAP-C114986-02) from Technology Advancement Research Program (TARP) funded by Ministry of Land, Infrastructure and Transport of Korean government.

Publisher's Note

Springer Nature remains neutral with regard to jurisdictional claims in published maps and institutional affiliations.

Received: 24 October 2017 Accepted: 2 May 2018

Published online: 02 August 2018

References

- Ashour, S. A. (2000). Effect of compressive strength and tensile reinforcement ratio on flexural behavior of high-strength concrete beams. *Engineering Structures*, 22(5), 413–423.
- Cheng, F. P., Kodur, V. K. R., & Wang, T. C. (2004). Stress-strain curves for high strength concrete at elevated temperatures. *Journal of Materials in Civil Engineering*, 16(1), 84–90.
- Choi, J., Haj-Ali, R., & Kim, H. S. (2012). Integrated fire dynamic and thermo-mechanical modeling of a bridge under fire. *Structural Engineering and Mechanics*, 42(6), 815–829.

- Choi, J., Kim, H., & Haj-Ali, R. (2010). Integrated fire dynamics and thermomechanical modeling framework for steel-concrete composite structures. *Steel and Composite Structures*, 10(2), 129–149.
- European Committee. (1995). Eurocode2: Design of concrete structures-Part 1-2: General rules-Structural fire design. EN 1992-1-2.
- Harmathy, T. Z. (1970). Thermal properties of concrete at elevated temperatures. *Journal of Materials*, 5(1), 47–74.
- Harmathy, T. Z. (1993). Fire safety design and concrete, Scientific and Technical.
- Hawileh, R. A., & Naser, M. Z. (2012). Thermal-stress analysis of RC beams reinforced with GFRP bars. *Composites Part B Engineering*, 43(5), 2135–2142.
- Hawileh, R. A., Naser, M., & Rasheed, H. A. (2011). Thermal-Stress finite element analysis of CFRP strengthened concrete beam exposed to top surface fire loading. *Mechanics of Advanced Materials and Structures*, 18(3), 172–180.
- Hawileh, R. A., Naser, M., Zaidan, W., & Rasheed, H. A. (2009). Modeling of insulated CFRP-strengthened reinforced concrete T-beam exposed to fire. *Engineering Structures*, 31(12), 3072–3079.
- Hsu, J. H., Lin, C. S., & Huang, C. B. (2006). Modeling the effective elastic modulus of RC beams exposed to fire. *Journal of Marine Science and Technology*, 14(2), 102–108.
- ISO 834. (1999). *Fire resistance tests—elements of building construction*. Switzerland: International Organization for Standardization.
- Jau, W. C., & Huang, K. L. (2008). A study of reinforced concrete corner columns after fire. *Cement and Concrete Composites*, 30(7), 622–638.
- Kang, J., Yoon, H., Kim, W., Kodur, V., Shin, Y., & Kim, H. (2016). Effect of wall thickness on thermal behaviors of RC walls under fire conditions. *International Journal of Concrete Structures and Materials*, 10(3), 19–31.
- Kodur, V. K. R., & Sultan, M. A. (2003). Effect of temperature on thermal properties of high-strength concrete. *Journal of Materials in Civil Engineering*, 15(2), 101–107.
- Lamont, S., Usmani, A. S., & Drysdale, D. D. (2001). Heat transfer analysis of the composite slab in the Cardington frame fire tests. *Fire Safety Journal*, 36(8), 815–839.
- Rashid, M. A., & Mansur, M. A. (2005). Reinforced high-strength concrete beams in flexure. *Structural Journal*, 102(3), 462–471.
- Ryu, E. M., An, A. Y., Kang, J. Y., Shin, Y. S., & Kim, H. S. (2015). Investigation of rehabilitation effects on fire damaged high strength concrete beams. *World Academy of Science, Engineering and Technology, International Journal of Civil, Environmental, Structural, Construction and Architectural Engineering*, 9(7), 898–904.
- Shin, Y. S., Park, J. E., Mun, J. Y., & Kim, H. S. (2011). experimental studies on the effect of various design parameters on thermal behaviors of high strength concrete columns under high temperatures. *Journal of the Korea Concrete Institute*, 23(3), 377–384.
- Sullivan, T. J., Calvi, G. M., & Priestley, M. J. N. (2004). Initial stiffness versus secant stiffness in displacement based design. In *13th World Conference on Earthquake Engineering*, 2888.
- Wu, B., Xiong, W., & Wen, B. (2014). Thermal fields of cracked concrete members in fire. *Fire Safety Journal*, 66, 15–24.

Submit your manuscript to a SpringerOpen® journal and benefit from:

- Convenient online submission
- Rigorous peer review
- Open access: articles freely available online
- High visibility within the field
- Retaining the copyright to your article

Submit your next manuscript at ► springeropen.com